Available online at www.sciencedirect.com
ScienceDirect
Polymer 47 (2006) 7406–7413
polymer
www.elsevier.com/locate/polymer

In situ characterization of moisture sorption/desorption in thin polymer films using optical waveguide spectroscopy

Li-Qiang Chu [a,b], Hai-Quan Mao [d], Wolfgang Knoll [a,b,c,*]

[a] *Max-Planck-Institut für Polymerforschung, Ackermannweg 10, 55128 Mainz, Germany*
[b] *Department of Materials Science and Engineering, National University of Singapore, Singapore 117576, Singapore*
[c] *Department of Chemistry, National University of Singapore, Singapore 117543, Singapore*
[d] *Department of Materials Science and Engineering, Johns Hopkins University, Baltimore, MD 21218, USA*

Received 17 May 2006; received in revised form 12 August 2006; accepted 16 August 2006
Available online 7 September 2006

Abstract

The kinetics of moisture sorption/desorption in poly(terephthalate-*co*-phosphate) thin films was investigated in situ at $T = 25\ ^{\circ}C$ using optical waveguide spectroscopy (OWS). At low water activities, Fickian diffusion was observed for the initial phase of the sorption process, while at high activities, due to the clustering of water, a complex sorption behavior was found. The moisture sorption isotherms were analyzed according to both the Zimm and Lundberg model as well as the Brown model, which suggests the formation of clusters of water molecules in poly(terephthalate-*co*-phosphate) at water activities of $\alpha_1 = 0.58$ or higher. The water diffusion coefficient decreases with increasing water activity, which also suggests water cluster formation. A biphasic desorption behavior was also observed upon decreasing the water activity from $\alpha_1 = 1$ to 0. This study demonstrated the unique advantages of OWS in characterizing in situ the sorption/desorption behavior of penetrants in polymer thin films.

Keywords: Moisture sorption/desorption; Optical waveguide spectroscopy; Poly(terephthalate-*co*-phosphate)

1. Introduction

Polymeric materials usually adsorb moisture when exposed to a humid atmosphere or immersed in aqueous media. The moisture sorption may affect the physical and chemical properties of polymers, such as the glass transition temperature (T_g), the mechanical strength, the gas permeation behavior, etc [1–5]. A great deal of efforts thus were put into the studies of water vapor sorption and diffusion in polymer matrixes, particularly for polymeric materials employed in an aqueous environment, such as in food packing, for gas separation, controlled drug release, biomedical applications, as polymeric adhesive, etc.

Since water molecules can interact strongly not only with the polymer matrix but also with themselves via hydrogen bonding, the state of water within the polymer matrix depends on the extent of water–polymer interaction, as well as on the water activities (i.e., on the relative humidity). At lower water activities, water is distributed mainly within the polymer matrix, physisorbed to active sites via hydrogen bonds. This can generally be described by the Flory–Huggins solution theory. At higher activities, water has a tendency to cluster or to cause plasticization of the polymer matrix depending on the possibility of forming hydrogen bonds among water molecules, or between water and hydrophilic groups. Three types of water have been proposed to exist in a polymer matrix. Primary bound water (Type III) is strongly associated with polar groups of the polymer chains. Secondary bound water (Type II) is hydrophobically bound water formed at high humidity through water–water hydrogen bonds. Bulk water (Type I) is solvent-like water, which is similar to that of bulk water in aqueous solution.

* Corresponding author. Max-Planck-Institut für Polymerforschung, Ackermannweg 10, 55128 Mainz, Germany. Tel.: +49 6131 379161; fax: +49 6131 379360.
E-mail address: knoll@mpip-mainz.mpg.de (W. Knoll).

0032-3861/$ - see front matter © 2006 Elsevier Ltd. All rights reserved.
doi:10.1016/j.polymer.2006.08.031

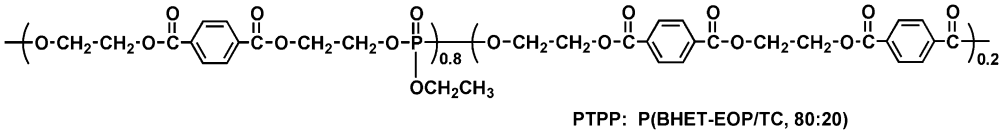

Fig. 1. The chemical structure of poly(terephthalate-*co*-phosphate).

Recently, a new polyphosphoester co-polymer, namely P(BHET-EOP/TC), was developed in order to obtain not only the typical biodegradable characteristics of polyphosphoester but also to have strong mechanical properties by incorporating phosphates into the poly(ethylene terephthalate) (PET) backbone [6]. In contrast to PET, the co-polymer is more amorphous. The flexible phosphoester bonds in the backbone lower the glass transition temperature and confer good solubility in common solvents, e.g., chloroform. The pentavalency of the phosphorus atom in the backbone allows for chemical linkage of other molecules to the polymer. With an EOP/TC ratio of 80:20, the co-polymer showed a favorable toxicity profile in vitro and good tissue biocompatibility [6]. It was suggested that this class of biodegradable co-polymers may find use in biomedical applications, such as drug delivery and tissue engineering. In this work, we will investigate the moisture sorption/desorption behavior of this new co-polymer.

Optical waveguide spectroscopy had proved to be well suited to characterize polymer thin films ranging from several hundred nanometers to a few micrometers in thickness [7–9]. For example, the behavior of PMMA films at various temperatures and pressures was studied using this optical technique [10–12]. It was also applied successfully to monitor the kinetics of the swelling of polymer brushes [13,14] and plasma polymerized thin films [15]. OWS can determine the (isotropic) refractive index (n) and the thickness (d) simultaneously, provided at least two modes can be guided in the thin film structure.

In this report, OWS was employed to monitor in situ the kinetic behavior of moisture sorption and desorption in thin films of P(BHET-EOP/TC). The P(BHET-EOP/TC) films were spin-coated to a thickness of ca. 500 nm, which allowed for exciting at least two waveguide modes in an OWS spectrum. It provided sufficient data for simultaneous determination of the thickness and the refractive index of the thin film. The moisture sorption isotherm was obtained from the thickness of the swollen P(BHET-EOP/TC) films at a given relative humidity, which was then analyzed using different models, including the Flory–Huggins model, the Zimm and Lundberg model and Brown model. Our results suggest that water molecules tend to form clusters in the polymer matrix at high water activity.

2. Experimental

2.1. Materials

The synthesis of P(BHET-EOP/TC, 80:20) was described in details before [6]. The ratio in the notation refers to the molar ratio of EOP to TC units in the polymer backbone. Its chemical structure is given in Fig. 1. In brief, 1,4-bis(2-hydroxyethyl)terephthalate (BHET) was first reacted with ethyl phosphorodichloridate (EOP) to yield a hydroxyl-terminated prepolymer, which was further polymerized with terephthaloyl chloride (TC). Milli-Q water was used throughout the experiments. LaSFN9 glass slides ($n = 1.844$ at $\lambda = 633$ nm, Hellma Optik, Jena, Germany) were used in the OWS measurements. The LaSFN9 slides were cleaned with 2% Hellmanex detergent, rinsed extensively with water, then with ethanol, and finally dried thoroughly with pure nitrogen gas. A 2-nm chromium layer and a 50-nm gold layer were deposited onto the glass slides. Here the chromium layer is used to enhance the adhesion of gold on the LaSFN9 glass. The P(BHET-EOP/TC, 80:20) polymer was dissolved in chloroform at a concentration of 2 wt%, and was then spin-coated onto Au coated LaSFN9 slides at 2000–3000 rpm resulting in a thickness of 400–600 nm. Prior to the OWS measurements, the films were dried at 50 °C for 24 h in order to remove any solvent from the film.

2.2. Optical waveguide spectroscopy (OWS)

The use of OWS for the characterization of thin films has already been discussed in details elsewhere [7–9]. The OWS scan can be fitted using the Fresnel equations obtaining not only the refractive index n but also the thickness d of the guiding film provided at least two optical modes can be excited. The excitation of waveguide modes can be achieved not only by p-polarized light but also by s-polarized light allowing for the characterization of optically anisotropic films. OWS measurements were carried out with a home-built setup based on the Kretschmann configuration (as shown in Fig. 2) as described before [7,13]. The samples were mounted to a Teflon cell, which could be kept at a constant relative humidity. The humidity inside the Teflon cell was controlled by using a small vessel filled with a saturated aqueous salt solution in contact with excess salt. The high salt content of the solution reduces the water vapor pressure to a distinct value. Saturated salt solutions of lithium bromide, calcium chloride, potassium carbonate, sodium bromide, sodium chloride, potassium chloride, zinc sulfate were used to achieve a desired humidity, i.e., 6%, 29%, 43%, 58%, 75%, 84%, 90%, respectively [13,15]. Zero humidity was obtained by drying the samples over potassium hydroxide pellets. One hundred percent humidity was obtained through pure H_2O. Each sample was firstly dried with solid potassium hydroxide before introducing the salt solution. During the moisture exposure, the change in thickness was monitored by measuring the shift in the minimum dip of

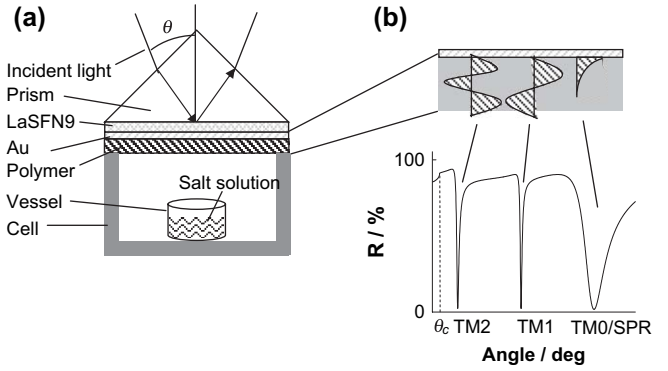

Fig. 2. (a) Schematic of sample installation in OWS (Kretschmanns configuration) accompanied with a humidity cell, into which a vessel containing the saturated salt solution was placed and (b) the schematic of waveguide modes within the polymer film, which can be seen in the reflectivity curve if one measures the reflectivity as a function of incident angle.

a waveguide mode as a function of time. The time resolution is better than 1.5 s. Once equilibrium of the swelling process was reached, an OWS angular scan was taken in order to determine the thickness and the refractive index of the swollen polymer.

3. Results and discussion

3.1. OWS measurement

Moisture sorption of P(BHET-EOP/TC) films at controlled water activity was monitored using OWS accompanied with a specific cell, to which the sample was attached. A small vessel containing either solid KOH pellets or saturated salt solutions was placed into the cell in order to obtain desired water activity. For determination of the thickness of P(BHET-EOP/TC) at various water activities, the reflectivity versus the incident angle curves were recorded at a constant temperature. Fig. 3 shows the typical reflectivity versus incident angle curve for P(BHET-EOP/TC) at water activities of 0, 0.75 and 1. It is evident that two waveguide modes could be excited and after

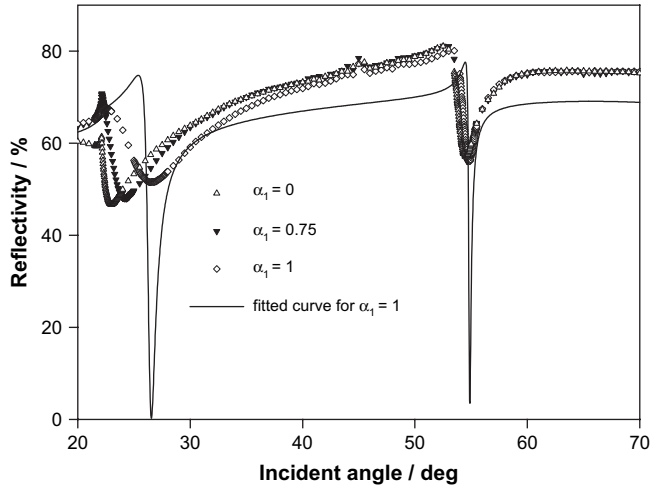

Fig. 3. Typical s-polarized OWS spectra of a P(BHET-EOP/TC) film at various water activities, $T = 25$ °C.

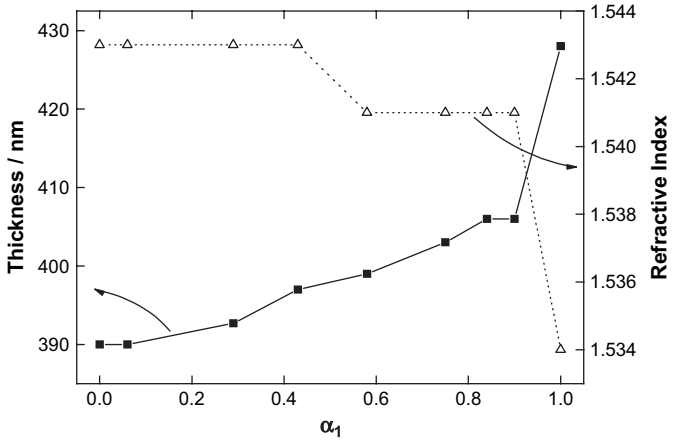

Fig. 4. The thickness and the refractive index of a P(BHET-EOP/TC) film for various water activities.

introducing the humid air, the higher order mode located at lower incident angles is shifted to higher angles. This indicates a large increase in thickness of the P(BHET-EOP/TC) film due to the swelling by incorporation of water molecules into the polymer matrix. The reflection curve can be fitted based on Fresnel equation using a simple box model. Because of the presence of two waveguide modes, both the thickness and the refractive index of P(BHET-EOP/TC) at various water activities were determined independently, which is shown in Fig. 4. Clearly, with increasing water activity, the thickness of the P(BHET-EOP/TC) film increases due to the swelling induced by the incorporation of water molecules.

3.2. Flory–Huggins analysis

For a flat sheet, the relative increase in thickness is directly proportional to the change in volume. Consequently, the relative increase in P(BHET-EOP/TC) thickness can be used to calculate the volume fraction ϕ_1 of water within the polymer:

$$\phi_1 = \frac{d_{eq} - d_0}{d_{eq}} = 1 - \frac{d_0}{d_{eq}} \quad (1)$$

here d_0 is the thickness of the film at $\alpha_1 = 0$, and d_{eq} is the equilibrium thickness of the film at various water activities. The water uptake as indicated by the volume fraction is 3.9% and 8.9% for P(BHET-EOP/TC) at $\alpha_1 = 0.9$ and $\alpha_1 = 1$, respectively. It is very surprising that there is a 'jump' in P(BHET-EOP/TC) thickness at $\alpha_1 = 1$ compared to that at $\alpha_1 = 0.9$. The incorporation of water molecules ($n = 1.333$) into the P(BHET-EOP/TC) layer ($n = 1.543$) also results in a decrease in the refractive index, as can be seen in Fig. 4. At $\alpha_1 = 1$ a refractive index of $n = 1.534$ was obtained indicating approximately 4.3% water incorporation into the film. This water uptake value is higher than that for PET, which can only adsorb 1% or less of water. The reason is that P(BHET-EOP/TC) is hydrophilic compared to PET because of the incorporation of phosphate in the backbone.

In Fig. 5 the volume fraction ϕ_1 of water sorbed in P(BHET-EOP/TC) at 25 °C is shown as a function of the water

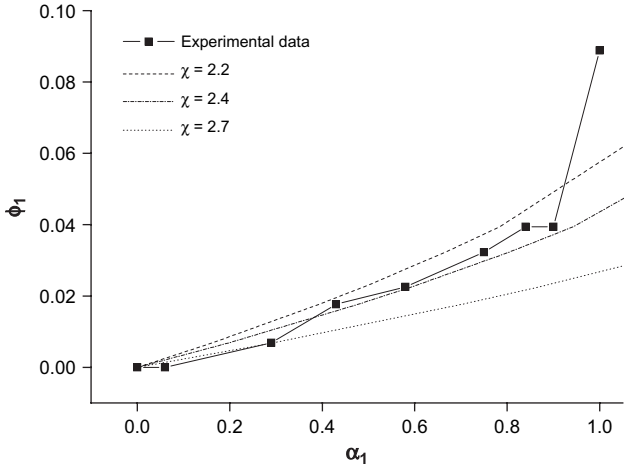

Fig. 5. The volume fraction of water within the P(BHET-EOP/TC) film as a function of water activities. The lines are the simulations according to the Flory–Huggins equation. The different interaction parameters used for the simulation are given in the figure.

activity α_1. This isotherm shows an upward curvature at low water activities and a big upturn at $\alpha_1 = 1$ (i.e., 100% relative humidity). The sorption isotherm was firstly correlated according to conventional solution thermodynamics, i.e., the Flory–Huggins theory [16–18]:

$$\alpha_1 = \phi_1 \exp\left((1-\phi_1) + \chi(1-\phi_1)^2\right) \tag{2}$$

where α_1 is the water activity, ϕ_1 is the volume fraction of water in the polymer, and χ is the Flory–Huggins interaction parameter. By fitting the experimental data using Eq. (2), it is possible to calculate the Flory–Huggins interaction parameter χ. The χ value provides a good indication of the solvent power as a penetrant for the polymers. The lines in Fig. 5 represent the calculated curves from Eq. (2) using different interaction parameters χ as indicated in the figure. Clearly, the value at $\alpha_1 = 1$ is out of the fitting range and the Flory–Huggins model cannot describe the whole sorption isotherm of the present case. However, by comparing the simulated curves with the measured data at low water activities, $\alpha_1 < 0.9$, the Flory–Huggins interaction parameter χ is estimated to be in the range between 2.2 and 2.7. The high value of interaction parameter χ indicates that the interaction of water molecules with each other is stronger than the interaction between water and the polymer segments. Water is still not a good solvent of P(BHET-EOP/TC) even though more polar groups exist in P(BHET-EOP/TC) than in PET.

The curvature and strong upturn observed in the sorption isotherm may be caused by two phenomena: (1) the clustering of water molecules [17,19,20], or (2) the plasticization of the polymer matrix induced by water sorption [21,22]. Clustering causes an increase in the average size of a water molecule and hence reduces the diffusion coefficient, while plasticization allows the polymer chains to move more freely leading to faster diffusion. Thus the behavior of the diffusion coefficient can be used to differentiate between plasticization and clustering. In this study, the diffusion coefficient decreases with increasing humidity (given in Section 3.5), indicating clustering of water molecules as the predominant process for sorbed water, particularly at high water activities. Two independent methods were employed for the clustering analysis: (1) the Zimm and Lundberg theory [23], and (2) the Brown theory [24].

3.3. Zimm and Lundberg analysis

Zimm and Lundberg [23] developed a mathematical approach to determine the tendency of penetrant molecules to cluster in a polymer based on a quantity called the cluster integral, G_{11}, which can be obtained directly from equilibrium data using the equation:

$$\frac{G_{11}}{\nu_1} = -(1-\phi_1)\left[\frac{\partial\left(\frac{\alpha_1}{\phi_1}\right)}{\partial\alpha_1}\right]_{P,T} - 1 \tag{3}$$

here, ν_1 is the partial molar volume of the penetrant, α_1 is the penetrant activity, ϕ_1 is the volume fraction of the penetrant. P and T are the pressure and temperature, respectively. The quantity G_{11}/ν_1 is a measure of the tendency of penetrant molecules to form clusters. For an ideal solution, G_{11}/ν_1 is equal to -1 because the activity α_1 is proportional to the volume fraction ϕ_1. If $G_{11}/\nu_1 < -1$, penetrant molecules (water in the present study) prefer to remain isolated. If $G_{11}/\nu_1 > -1$, penetrant molecules tend to cluster. If $G_{11}/\nu_1 = 0$, the degree of clustering is just sufficient to overcome the excluded volume of the polymer molecule. The extent of clustering is indicated by the extent to which G_{11}/ν_1 exceeds -1.

Zimm and Lundberg [23] have provided a more useful quantity $\phi_1 G_{11}/\nu_1$, which refers to the mean number of excess water molecules in the neighborhood of a given water molecule. This definition specifies the excess water molecules in the vicinity of the central water molecule, but does not include the central water molecule. If the water solvent molecule is included, Brown [24] has suggested that the average number of water molecules in a cluster (N_c, the so called cluster number) can be calculated by the following equation:

$$N_c = \phi_1\left(\frac{G_{11}}{\nu_1} + 1\right) + 1 \tag{4}$$

and

$$N_c = -\phi_1(1-\phi_1)\left[\frac{\partial\left(\frac{\alpha_1}{\phi_1}\right)}{\partial\alpha_1}\right] + 1 \tag{5}$$

For an ideal solution, there is no clustering and N_c is equal to 1.

The Jones method [2,25] can be employed to solve the differential in Eq. (3). If α_1/ϕ_1 is plotted against α_1, the experimental data can be fitted according to second order polynomial, which is then differentiated. In this analysis, a small term of the compressibility of the penetrant in a binary mixture is ignored. The results of Zimm and Lundberg analysis are shown in Table 1. The data at $\alpha_1 > 0.43$ were used in the curve

Table 1
The results of Zimm and Lundberg analysis

RH (%)	α_1	ϕ_1	α_1/ϕ_1	G_{11}/v_1	N_c
43	0.43	0.018	24.4	−30.3	0.48
58	0.58	0.023	25.7	−4.6	0.92
75	0.75	0.032	23.2	22.9	1.77
84	0.84	0.039	21.3	38.6	2.56
90	0.9	0.039	22.8	47.7	2.92
100	1	0.089	11.3	60.3	6.44

fitting because clustering of water molecules may occur preferably at higher water activity. From Table 1, it can be seen that at $\alpha_1 < 0.58$, the cluster integral G_{11}/v_1 is lower than -1, indicating that water molecules are randomly mixing within the polymer. While at $\alpha_1 > 0.75$, the cluster integral, G_{11}/v_1, is higher than -1, which suggests a high tendency of water cluster formation. The calculated cluster number N_c also shows the same trend. At $\alpha_1 = 0.9$, water forms clusters with an average number of 2.9 water molecules. If the humidity is increased to $\alpha_1 = 1$, water forms clusters composed of an average of 6.4 water molecules. The P(BHET-EOP/TC) used in this work is largely amorphous and the distribution of phosphate groups in the backbone is relatively random throughout the polymer chain [6]. At low α_1, water is distributed throughout the polymer matrix, probably in the form of primary bound water. As α_1 increases, clustering of water molecules (secondary bound water) gradually becomes the predominant form of water.

3.4. Brown analysis

Brown [24] has proposed a method to analyze the water sorption into certain polar polymers. In his model the conventional Flory–Huggins theory and cluster theory are combined, and the total water sorbed by a polymer is viewed as the sum of the fractions of randomly distributed water molecules (Flory–Huggins solution theory) and non-randomly mixing water molecules, e.g., clusters. In Brown analysis, the reciprocal of volume fraction of the water is plotted against the reciprocal of the partial pressure of water, which can be described by the following equation:

$$\frac{1}{\phi_1} = \frac{K_1}{P_1} - K_2 \tag{6}$$

here P_1 is the partial pressure of water (i.e., water activity α_1). K_1 and K_2 are constants. For $K_2 = 0$, this equation corresponds to the sorption behavior described by Henry's law. If K_2 is negative the isotherm is considered to be a Langmuir or of an attenuated type. If K_2 is positive it is an enhanced cluster isotherm. As P_1 approaches zero, the infinite dilution isotherm is given by the inverse of Henry's law:

$$\frac{1}{\phi_H} = \frac{K_1}{P} \tag{7}$$

This analysis also provides a unique calculation of the Flory–Huggins interaction parameters, χ. Through the use of the limiting (Henry's law) approximation of the Flory–Huggins theory, χ can be defined according to equations:

$$P \approx \phi_1 \exp(1+\chi) \approx K_1 \phi_1 \tag{8}$$

and

$$\chi = \ln K_1 - 1 \tag{9}$$

At any relative pressure, the experimental sorption data can be compared to that predicted by Henry's law to provide a ratio, N_e, which is defined as the enhancement number and can be calculated from Eqs. (6) and (7):

$$N_e = \frac{\phi_1}{\phi_H} = \frac{K_1}{K_1 - K_2 P} = 1 + K_2 \phi_1 \tag{10}$$

The enhancement number is a measure of the extent to which the sorption of water is increased by the abnormalities of the process, which results from non-random mixing, e.g., clustered or associated water.

Using the partial pressure of water as an adequate approximation to the activity, it can be seen from Eq. (6) that the derivative within the brackets in Eq. (5) is equal to $-K_2$. Consequently, the cluster number can be calculated by equation:

$$N_c = 1 + K_2\phi_1 - K_2\phi_1^2 = N_e - K_2\phi_1^2 \tag{11}$$

Brown model was applied to the experimental sorption data of P(BHET-EOP/TC). Fig. 6 shows a plot of the reciprocal of the volume fraction ϕ_1 of water as a function of the reciprocal partial pressure of water, which exhibits a near-linear behavior for the data obtained at high pressures ($\alpha_1 > 0.29$). The results of the Brown analysis are given in Table 2. The calculated Flory–Huggins interaction parameter χ is 2.9, which is consistent with the estimated value ranging from 2.2 to 2.7 by the Flory–Huggins analysis. Both analyses showed that $\chi > 1$, suggesting that water is not a good solvent for P(BHET-EOP/TC). Therefore, it is reasonable that water molecules tend to form clusters in the P(BHET-EOP/TC) at high

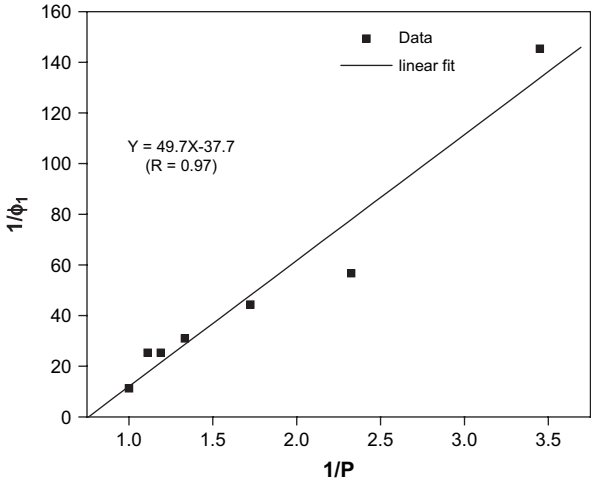

Fig. 6. Brown cluster analysis of the moisture sorption in a P(BHET-EOP/TC) film.

Table 2
The results of Brown analysis

K_1	K_2	χ	Value at $P=1$		
			ϕ_1	N_e	N_c
49.7	37.7	2.9	0.083	4.1	3.9

activity. The cluster number N_c at 100% RH is 3.9, which is lower than that obtained from Zimm and Lundberg analysis (Table 1).

3.5. Sorption kinetics

The kinetics of moisture sorption and desorption in P(BHET-EOP/TC) film can be monitored with OWS by measuring the angular position of one waveguide mode as a function of time. Fig. 7 shows the change of the first order waveguide mode ($m=1$, in p-polarized light OWS, data are not shown here) as a function of time. The P(BHET-EOP/TC) film was attached to a special cell in which KOH pellets guaranteed 0% humidity in equilibrium. Upon changing KOH with various saturated salt solutions (i.e., various relative humidities), the waveguide mode shifts to higher angles very quickly within the first several minutes and reaches equilibrium within about 10 min. The only exception is in the case of 100% relative humidity, which shows that the process is initially very fast while after ca. 2 min a secondary much slower process takes over, and equilibrium is reached only after about 5 h. Note that for $\alpha_1 < 0.43$, the minimum mode shifts to higher angle at first and then shifts back to equilibrium value. The huge shift at the beginning was caused by an experimental artifact. To change the vessel containing the salt solution, the cell had to be opened and the film was briefly exposed to ambient humidity (approximately 55–70% in our lab). For this reason, we analyzed the kinetic data for only $\alpha_1 > 0.58$ in the following part. The fast process may represent diffusion of water molecules into P(BHET-EOP/TC) followed by clustering of water molecules within the film. The sample had always been dried back to the starting thickness value in a 0% relative humidity before the next sorption experiments were started. It can be seen from Fig. 7 that the starting point of every curve is almost at the same level. This indicates that the moisture sorption and desorption of P(BHET-EOP/TC) are fully reversible.

Two characteristics features [26–28] of Fickian diffusion of a solvent in a polymer film are: (i) the plot of the fractional penetrant uptake M_t/M_∞ against the square root of the time is linear up to at least $M_t/M_\infty = 60\%$ for both adsorption and desorption and (ii) above the linear region, the sorption curves are concave to the abscissa. Here M_t is the mass of penetrant at time t, and M_∞ is the equilibrium mass. In this study, M_t/M_∞ can be calculated by the following relationship:

$$\frac{M_t}{M_\infty} = \frac{d_t - d_0}{d_{eq} - d_0} \tag{12}$$

We already found that the change of the refractive index of P(BHET-EOP/TC) is very small except for the value at 100% humidity. The minimum angle change in Fig. 7 can be correlated to the change in P(BHET-EOP/TC) thickness.

A plot of M_t/M_∞ versus $t^{0.5}/d_0$ for high water activities $\alpha_1 \geq 0.58$ is shown in Fig. 8. It can be found that the initial part (except first data point) exhibits a linear correlation for M_t/M_∞ up to 60% at all water activities, indicating that the sorption is described by a Fickian diffusion. The first data point is lower, as expected for Fickian diffusion. This may be an indication of a time lag, which was probably caused by the lower surface concentration compared to the equilibrium value. We collect the time data instantaneously after the saturated salt solution was placed into the OWS cell. It takes some time for the water activity in the OWS cell to reach equilibrium. As a result, a sigmoidal shape of the sorption curve is expected at the initial stage of the sorption [29].

From the initial slope of the curve in Fig. 8, it is also possible to obtain the average diffusion coefficient [28,29]. In the present work the water molecules penetrate into the films from one side of the films. Therefore, for a constant diffusion

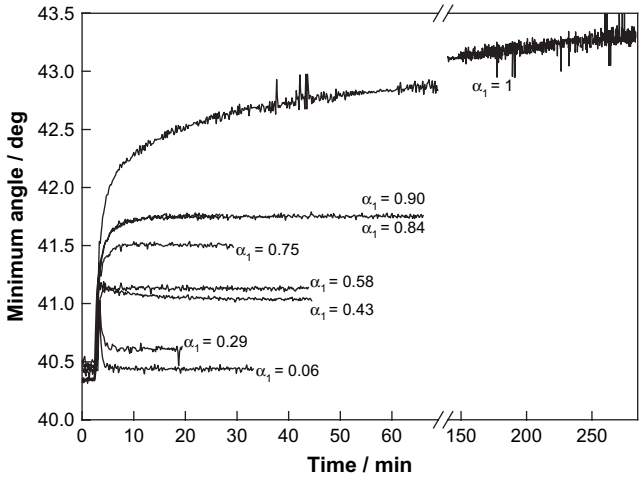

Fig. 7. Kinetics of moisture sorption into a P(BHET-EOP/TC) film at various water activities.

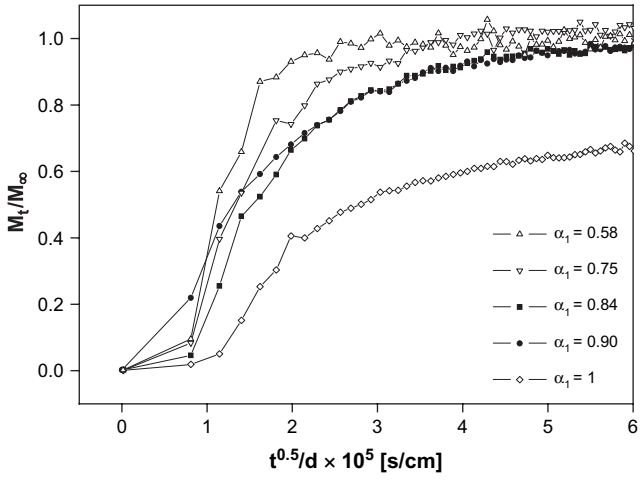

Fig. 8. A plot of M_t/M_∞ versus $t^{0.5}/d$ at various water activities.

coefficient D and a polymer film of thickness d, the diffusion equation can be expressed as:

$$\frac{M_t}{M_\infty} = \frac{2}{\pi^{0.5}} \left(\frac{Dt}{d^2}\right)^{0.5} \tag{13}$$

if the initial slope, $R = \partial(M_t/M_\infty)/\partial(t^{0.5}/d)$, is observed in a sorption experiment in which D is concentration dependent, the average diffusion coefficient can be deduced from Eq. (13) as:

$$D = \frac{\pi}{4}\left[\frac{\partial(M_t/M_\infty)}{\partial(t^{0.5}/d)}\right]^2 = \frac{\pi}{4}R^2 \tag{14}$$

The calculated diffusion coefficients are the averages for a concentration range from zero to the equilibrium value at a given activity. The diffusion coefficients calculated using Eq. (14) are given in Table 3. It can be seen that there is a decrease in the diffusion coefficient with increasing water activity, which suggests that clustering of water molecules dominates at high activity. Water clustering is associated with a diffusion coefficient that decreases with increasing water activity. This trend is in contrast to a plasticizing effect by which the diffusion coefficient normally increases with increasing solvent concentration.

In order to understand the nature of the diffusion process in P(BHET-EOP/TC), the initial portion of the sorption data was also fitted to an empirical equation:

$$\frac{M_t}{M_\infty} = kt^m \tag{15}$$

where the m value indicates the type of diffusion mechanism. Fickian diffusion is indicated by $m = 0.5$ [27]. If diffusion is very fast, m is equal to 1. The third case is anomalous diffusion with m values ranging between 0.5 and 1. For $\alpha_1 \geq 0.58$, $\ln(M_t/M_\infty)$ was plotted against $\ln(t)$, as shown in Fig. 9. Table 3 summarized the slope of all curves for the early data points excluding the first data point. Note the time range is identical to that in Fig. 8. At low humidity, they all are approximately $m = 0.5$, which confirms that the water diffusion into P(BHET-EOP/TC) is controlled by a Fickian diffusion behavior. But at 100% humidity, high value of $m = 1.18$ indicates that the water molecule diffuses much faster through the P(BHET-EOP/TC) layer than normal Fickian diffusion. At $\alpha_1 = 1$, the water molecules have strong tendency to cluster in P(BHET-EOP/TC). This is consistent with the earlier analysis.

Table 3
Diffusion coefficient and exponential m at various water activities

α_1	$D \times 10^{11}$ cm^2/s	m
0.58	6.64	0.47
0.75	3.38	0.56
0.84	2.15	0.50
0.9	1.68	0.39
1	1.34	1.18

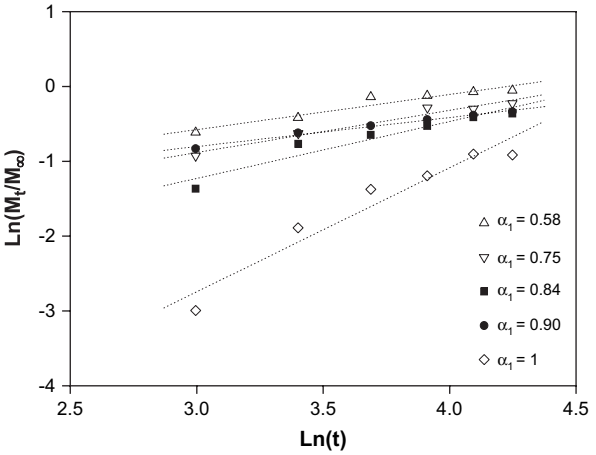

Fig. 9. A plot of $\ln(M_t/M_\infty)$ versus $\ln(t)$. The dotted lines are the linear fit of experimental data.

3.6. Desorption kinetics

We also monitor the moisture desorption from P(BHET-EOP/TC), as shown in Fig. 10. At $\alpha_1 = 0.9$ or lower, the minimum angle of the waveguide mode shifted back to the starting position very fast, which can be explained by Fickian diffusion. However, at $\alpha_1 = 1$, a biphasic desorption curve was observed showing a plateau between the two slopes. To the best of our knowledge, this is the first observation of this kind of desorption behavior. This is due to the high sensitivity of the OWS method: it is sensitive to small changes in the thin film thickness and has a high temporal resolution that can reach 1.5 s (10 s in this study). This temporal resolution is much higher than that of other traditional techniques, such as electromicrobalance. This biphasic desorption curve suggests that there are two types of water in a P(BHET-EOP/TC, 80:20) film, i.e., primary bound and secondary bound water. We hypothesized that the two step decrease in the desorption curve for $\alpha_1 = 1$ likely corresponds to two types of water in polymer film. The first decrease is the release of secondary bound water, and second slope corresponds to primary

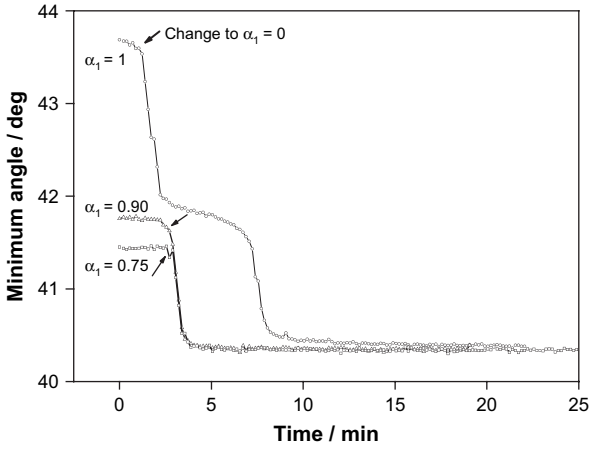

Fig. 10. Kinetics of moisture desorption from a P(BHET-EOP/TC) film at various water activities.

bound water. It is interesting to note that the second slope nearly overlaps the curve obtained for 90% RH. This may indicate that the same type of water exists at this phase (second peak for 100% RH curve) as that in the film at 90% RH. Nevertheless, a detailed analysis (such as near-IR [30], NMR) on the exact water state is needed to confirm this hypothesis.

4. Conclusions

Optical waveguide spectroscopy proved to be a sensitive technique for characterizing the kinetics of moisture sorption/desorption in polymer thin films. The moisture sorption isotherm can be obtained from the thickness change of the polymer film. Fickian diffusion is observed for the initial water sorption into P(BHET-EOP/TC) films. At high water activities, the majority of adsorbed water in P(BHET-EOP/TC) forms clusters (secondary bound water). A biphasic water desorption is observed for films equilibrated at 100% relative humidity. Zimm and Lundberg analysis of the sorption isotherms also suggests that water molecules form clusters in P(BHET-EOP/TC) films at high water activity. The water diffusion coefficient decreases with increasing activity, again, indicating water cluster formation rather than plasticization. It is worth noting that the optical technique used in the present study is widely applicable for investigating water sorption in polymer thin films, as the analysis does not require any predetermined parameters.

References

[1] Rowland SP. Water in polymers. Washington, DC: American Chemical Society; 1980.
[2] Karad SK, Jones FR. Polymer 2005;46:2732–8.
[3] Despond S, Espuche E, Cartier N, Domard A. J Polym Sci Part B Polym Phys 2005;43:48–58.
[4] Zhang Z, Britt IJ, Tung MA. J Polym Sci Part B Polym Phys 1998;37:691–9.
[5] Carfagna C, Apicella A. J Appl Polym Sci 1983;28:2881–5.
[6] Mao HQ, Shipanova-Kadiyala I, Zhao Z, Dang W, Brown A, Leong KW. J Biomater Sci Polym Ed 2005;16:135–61.
[7] Knoll W. Annu Rev Phys Chem 1998;49:569–638.
[8] Knoll W. In: Hummel RE, Wißmann P, editors. Handbook of optical properties II: optics of small particles, interfaces, and surfaces. Boca Raton: CRC Press; 1997. p. 373–400.
[9] Knoll W. MRS Bull 1991;16:29–39.
[10] Prucker O, Christian S, Bock H, Rühe J, Frank CW, Knoll W. Macromol Chem Phys 1998;199:1435–44.
[11] Kleideiter C, Lechner MD, Knoll W. Macromol Chem Phys 1999;200:1028–33.
[12] Fehrenbacher U, Jakob T, Berger T, Knoll W, Ballauff M. Fluid Phase Equilib 2002;200:147–60.
[13] Biesalski M, Rühe J. Langmuir 2000;16:1943–50.
[14] Biesalski M, Johannsmann D, Rühe J. J. Chem Phys 2002;117:4988–94.
[15] Chu LQ, Forch R, Knoll W. Langmuir 2006;22:2822–6.
[16] Flory PJ. Principles of polymer chemistry. London: Cornell University Press; 1953.
[17] Barrie JA, Machin D. Trans Faraday Soc 1971;67:244.
[18] Naylor T. Comprehensive polymer science, vol. 2. Elmsford, NY: Pergamon Press; 1989. p. 643.
[19] Barrie JA, Machin D, Nunn A. Polymer 1975;16:811–4.
[20] Barrie JA, Machin DJ. Macromol Sci Phys 1969;B3:645.
[21] Kelkar AJ, Paul DR. J Membr Sci 2001;181:199–212.
[22] Schult KA, Paul DR. J Polym Sci Part B Polym Phys 1996;34:2805–17.
[23] Zimm BH, Lundberg JL. J Phys Chem 1956;60:425–8.
[24] Brown GL. In: Rowland SP, editor. Water in polymers, vol. 127. Washington, DC: American Chemical Society; 1980. p. 441.
[25] Jacobs PM, Jones FR. J Mater Sci 1990;25:2471–5.
[26] Fujita H. In: Crank J, Park GS, editors. Diffusion in polymers. London: Academic Press; 1968. p. 75.
[27] Neogi P. In: Neogi P, editor. Diffusion in polymers. New York, NY: Marcel Dekker; 1996. p. 173.
[28] Rogers CE. In: Comyn J, editor. Polymer permeability. London: Elsevier; 1985. p. 11.
[29] Crank J. The mathematics of diffusion. Oxford: Clarendon; 1975.
[30] Mijovic J, Zhang H. Macromolecules 2003;36:1279–88.